PD Control and Sliding Mode Control Using Feedback Linearization for 3-Pole Radial Magnetic Bearings of an Energy Storage Flywheel *

David Cantero Burgos, Gabriel Mihai Sîrbu, Fernando Martin Porres,
Javier Vadillo Landajuela, Luis Fontan Agorreta

Dept. of Industrial Electronics
CEIT and Tecnun (University of Navarra)
Manuel de Lardizábal 15, 20018 San Sebastián, Spain
dcantero@ceit.es, gsirbu@ceit.es, fmartin@ceit.es, jvadillo@ceit.es, fontan@ceit.es

***Abstract* – In this paper a model and two control strategies are developed for the two radial active magnetic bearings (AMB) of an energy storage flywheel. The model is detailed, taking account of all significant phenomena in system. A linear control (proportional derivative control – PD control) and a nonlinear control (sliding mode control – SM control) based on the feedback linearization of the nonlinear magnetic bearing system are developed in order to find the best control for this system.**

***Index Terms* – 3-pole magnetic bearings, model, feedback linearization, linear control, sliding mode control.**

I. Introduction

In recent years energy storage flywheels have found wide applications in many areas such as uninterruptible power supplies (UPS), systems for power quality in power networks, improvement of the performance in wind generation systems and to avoid electric consumption peaks in high speed railway substations.

Moreover flywheels promise an alternative to chemical batteries for space systems like artificial satellites because of their higher efficiency in terms of energy per mass and volume, and have become an important area of research for use in electric/hybrid vehicles.

Main advantages of this technology are high energy density, long life, 90% depth of discharge and pulse power capability.

Due to high rotation speed, energy flywheel systems use active magnetic bearings (AMBs) to provide non-contact suspension, which is necessary to minimize the friction losses and to achieve long life and maintenance free systems.

Most of the magnetic radial bearings use the 8-pole arrangement because with this structure the magnetic flux coupling effects are neglected. In this case the force on each pair of poles can be express as a function of their own currents and the system can be modeled by two uncoupled one degree of freedom (DOF) systems. Each 1-DOF system can be linearized and many linear control methods can be applied to this model in order to obtain desired behavior (see [7]).

However the 8-pole arrangement impose the use of at least four independent power amplifiers, one for each pair of poles, and has the disadvantage of large energy losses.

In present paper a 3-pole radial magnetic bearing is considered. The 3-pole arrangement has the advantage of lower power losses, inferior number of power amplifiers and much more space for heat dissipation and to place coils and sensors. It seems the best way to achieve a low cost magnetic bearing system (see [1], [6]).

Nevertheless a 3-pole system is inherent nonlinear and the flux coupling effects can't be neglected. In the present paper feedback linearization technique with a linear control and a sliding mode control are considered.

II. System description

The experimental prototype has been developed together with the companies Elytt Energy and Antec S.A. which are members of the present investigation project.

This first prototype is intended to be an initial test for radial AMBs, but the goal is to achieve a full functionality kinetic storage system.

Fig.1a shows the system overview, and in Fig.1b the radial magnetic bearing can be observed. The radial bearing has a 3-pole structure with 3 coils connected in star.

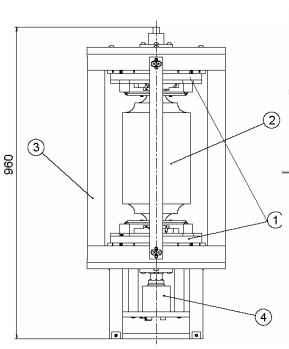

Fig.1a System overview (1-Radial AMB, 2-Flywheel, 3-Frame, 4-Air Turbine)

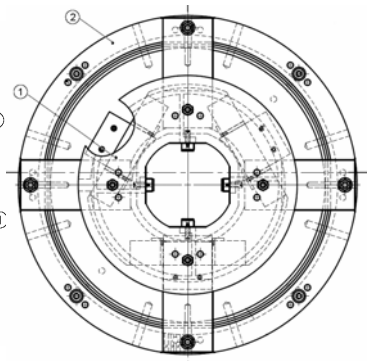

Fig.1b 3-Pole Radial Magnetic Bearing (1-Coil, 2-Magnetic Yoke)

* This work is partially supported by Basque Government INTEK research program and by Ministry of Science and Education and European Social fund "Torres Quevedo" grant.

The star connection of the coils let us use a 3-phase bridge inverter to power the system. The inverter is a 3-phase IGBT bridge with a 125VDC Bus and it can provide up to 40A in order to get about 800N force. The control stage has sensors to check the phase currents, the VDC Bus voltage and the position of the shaft and it uses a fixed point Motorola DSP56F803BU80E processor where the different control algorithms were implemented. The flywheel has 30kg and it has been designed to rotate at 30.000rpm storing 4 MJ of energy. It uses an air-turbine to move the shaft, but a reluctance motor is considered to be connected to the system in order to reach 30.000rpm and to provide a 100kW power for 20s when it will work like a generator.

III. Model of 3-pole AMB

In order to derive a model of 3-pole magnetic bearings the following assumptions are introduced:

- No dispersion flux, all flux lines are closing from iron circuit to air gap.
- Saturation curve is approximate by two segments (linear to saturation point and then the value is limited to that value).
- Magnetic fields are constant in a section.
- The air gap is constant along pole end.

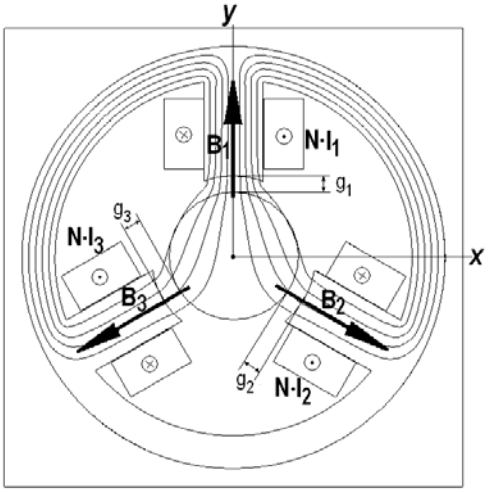

Fig 2. Magnetic circuit of the 3-pole AMB

Based on these hypotheses and the structure of magnetic bearings which provides magnetic flux coupling between coils the following independent equations are used (see Fig. 2):

$$\begin{aligned} &B_2 g_2 - B_1 g_1 = \mu_0 N(i_1 - i_2) \\ &B_3 g_3 - B_2 g_2 = \mu_0 N(i_2 - i_3) \\ &B_1 + B_2 + B_3 = 0 \end{aligned} \quad (1)$$

Where: g_1, g_2, g_3 – air gaps between rotor and poles; N - number of coil turns; μ_0 - magnetic permeability of the air; B_1, B_2, B_3 – magnetic field in air gaps; i_1, i_2, i_3 – currents in coils.

Air gaps depend on shaft position as follows:

$$\begin{aligned} g_1 &= g_0 - y \\ g_2 &= g_0 + y/2 - x\sqrt{3}/2 \\ g_3 &= g_0 + y/2 + x\sqrt{3}/2 \end{aligned} \quad (2)$$

Where: g_0 - nominal air gap; x, y - rotor displacement from center in Cartesian reference;

The star connection of coils gives the equation:

$$i_1 + i_2 + i_3 = 0 \quad (3)$$

i_3 current is replaced by $i_3 = -i_1 - i_2$, in all equations.

The following equations are obtained for magnetic fields B_1, B_2, and B_3 by solving system (1) and using (3):

$$\begin{aligned} B_1 &= L_1 i_1 + M_1 i_2 \\ B_2 &= M_2 i_1 + L_2 i_2 \\ B_3 &= L_3 i_1 + M_3 i_2 \end{aligned} \quad (4)$$

Where new parameters introduced are:

$$\begin{aligned} L_1 &= -\mu_0 N(2g_2 + g_3)/D_g & M_1 &= \mu_0 N(g_3 - g_2)/D_g \\ L_2 &= -\mu_0 N(2g_1 + g_3)/D_g & M_2 &= \mu_0 N(g_3 - g_1)/D_g \\ L_3 &= \mu_0 N(2g_2 + g_1)/D_g & M_3 &= \mu_0 N(2g_1 + g_2)/D_g \end{aligned} \quad (5)$$

Where $D_g = g_1 g_2 + g_2 g_3 + g_1 g_3$.

Voltage equations for the three coils (Y connection) are:

$$v_k - R_k i_k + N\frac{d\varphi_k}{dt} - v_N = 0 \quad k = 1,2,3 \quad (6)$$

Where v_1, v_2, v_3 - phases voltages; R_1, R_2, R_3 - coils resistances; φ_1, φ_2, φ_3 - coils fluxes; v_N - star point voltage.

Induced voltages in coils are described by the following:

$$N\frac{d\varphi_k}{dt} = NA\left(\frac{\partial B_k}{\partial I_1}\frac{di_1}{dt} + \frac{\partial B_k}{\partial I_2}\frac{di_2}{dt} + \frac{\partial B_k}{\partial x}\frac{dx}{dt} + \frac{\partial B_k}{\partial y}\frac{dy}{dt}\right) \quad (7)$$
$$k = 1,2,3$$

Where: A – pole area; N - number of coil turns;

Using (4) in (7) and then replacing (7) in (6) the voltage equations of the coils (6) become:

$$\begin{aligned} &NA\left(L_1\frac{di_1}{dt} + M_1\frac{di_2}{dt}\right) - v_N = -v_1 + R_1 i_1 - v_{B_1} \\ &NA\left(M_2\frac{di_1}{dt} + L_2\frac{di_2}{dt}\right) - v_N = -v_2 + R_2 i_2 - v_{B_2} \\ &NA\left(L_3\frac{di_1}{dt} + M_3\frac{di_2}{dt}\right) - v_N = -v_3 - R_3(i_1 + i_2) - v_{B_3} \end{aligned} \quad (8)$$

Where we defined:

$$v_{B_k} = NA\left(\frac{\partial B_k}{\partial x}\frac{dx}{dt} + \frac{\partial B_k}{\partial y}\frac{dy}{dt}\right) \quad k = 1,2,3 \quad (9)$$

These terms are in fact induced voltages by the movement of the shaft. These voltages are small and they can be neglected, but we considered them in our model. They are obtained using (4) and (5).

The following C_1, C_2, C_3 variables are defined to an easier calculus:

$$C_k = -v_k + R_k i_k - v_{B_k} \quad k = 1,2,3 \tag{10}$$

System (8) is solved for the currents derivates di_1/dt , di_2/dt and v_N. Currents derivates obtained and mechanical equations lead to the following model of the 3-pole magnetic bearing:

$$\begin{aligned}
\frac{di_1}{dt} &= \frac{1}{\Delta}\left[L_2(C_3 - C_1) + M_1(C_2 - C_3) + M_3(C_1 - C_2)\right] \\
\frac{di_2}{dt} &= \frac{1}{\Delta}\left[(L_1(C_3 - C_2) + M_2(C_1 - C_3) + L_3(C_2 - C_1))\right] \\
\frac{d^2x}{dt^2} &= \frac{F_x - F_{Rx}}{m} \\
\frac{d^2y}{dt^2} &= \frac{F_y - F_{Ry}}{m}
\end{aligned} \tag{11}$$

where: $\Delta = (NA)\left[L_1(M_3 - L_2) + L_3(L_2 - M_1) + M_2(M_1 - M_3)\right]$ and m – total mass of the rotor; F_x , F_y – bearing forces; F_{Rx} , F_{Ry} – resistive forces in x and y directions.

Bearing forces are calculated according with (4) and the following equations:

$$\begin{aligned}
F_x &= \frac{A}{2\mu_0}\left[B_2^2\cos(\pi/6) - B_3^2\cos(\pi/6)\right] \\
F_y &= \frac{A}{2\mu_0}\left[B_1^2 - B_2^2\cos(\pi/3) - B_3^2\cos(\pi/3)\right]
\end{aligned} \tag{12}$$

Equations (5), (9), (10), (11) and (12) make up the model of 3-pole magnetic bearing. Resistive forces F_{Rx} , F_{Ry} are developed according to mechanical behavior of this specific flywheel.

Saturation of the magnetic circuits was introduced as a limit of the magnetic fields. Because of coupled magnetic circuits, if one of the three magnetic fields reach the saturation value all three magnetic fields are limited to their actual values.

As the model is quite complex a block diagram of the model is showed in Fig. 3. The numbers in brackets specify equations used.

This model was used to simulate different controls, different behaviors of the system and losses.

The model can be simplified using magnetic fields equation, $B_1 + B_2 + B_3 = 0$, and B_3 can be replaced in all equations by:

$$B_3 = -B_1 - B_2 \tag{13}$$

In this case L_3 and M_3 parameters are not necessary.

IV. Feedback Linearization

The 3-pole AMB is a nonlinear system. In order to develop a control for this system, the current model is considered because it is less complex than the voltage one described above (see [2], [6]). According to the model developed (see block diagram in Fig. 3) and using equation (13) in order to simplify the model, the block diagram of the current model is the following:

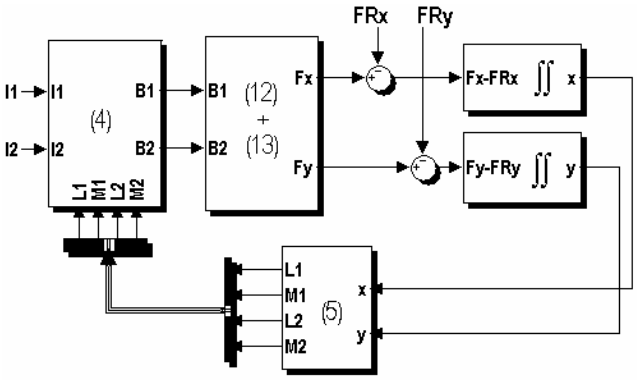

Fig. 4 Block diagram of the current model

The numbers in brackets specify equations used. Saturation is neglected.

The diagram presented above (Fig. 4) suggests two possible approaches of a control. First one is to consider a linear system around the operating point x=0, y=0, which means to neglect the loop and to consider a linear dependence between currents and magnetic fields in (4), without any dependence of the position as in [5].

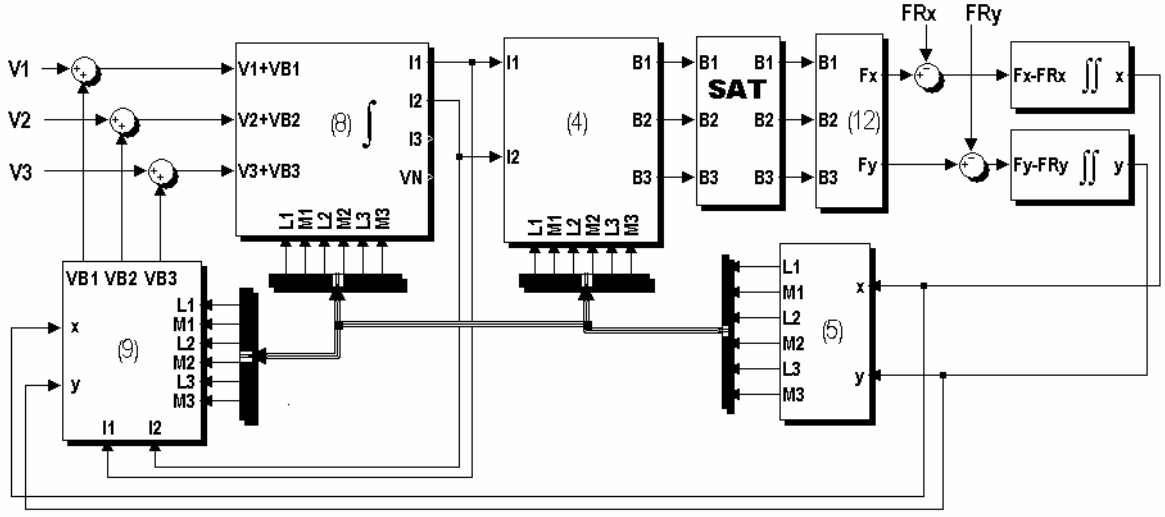

Fig. 3 Block diagram of the 3-pole AMB model

The control will have to decouple the two magnetic fields from forces in (12)+(13) block, in order to obtain a simple linear system. The second approach is to develop an exact feedback linearization loop which will cancel the nonlinear block (4) (in Fig.4) and with the same decoupling from magnetic fields and forces in (12)+(13), will lead to the same simple linear system as the first approach. We are going to present the second approach.

The current feed 3-pole AMB nonlinear system is described by the following state equations:

$$\begin{cases} \dot{\mathbf{x}} = f(\mathbf{x},\mathbf{i}) \\ \mathbf{y} = \mathbf{C}\cdot\mathbf{x} \end{cases} \tag{14}$$

Where the state variables $\mathbf{x} = [x_1, x_2, x_3, x_4]^{\mathrm{T}}$, are:

$x_1 = x$, $x_2 = \dot{x}_1 = \dot{x} = v_x$, $x_3 = y$, $x_4 = \dot{x}_3 = \dot{y} = v_y$,

v_x, v_y – shaft speed in x and y direction.

The input vector is current vector $\mathbf{i} = [i_1, i_2]^{\mathrm{T}}$, the output vector is position vector $\mathbf{y} = [x_1, x_3]^{\mathrm{T}} = [x, y]^{\mathrm{T}}$ and output matrix is $\mathbf{C} = [1 \quad 0 \quad 1 \quad 0]$.

By replacing B_1, B_2 from (4) in (12) and (13) we obtain the following form of the nonlinear system (14):

$$f(\mathbf{x},\mathbf{I}) = \begin{bmatrix} x_2 \\ \dfrac{A\sqrt{3}}{4m\mu_0}\begin{bmatrix} -i_1^2\left(L_1^2 + 2L_1M_2\right) - \\ 2i_1i_2\left(L_1M_1 + L_1L_2 + M_1M_2\right) - \\ i_2^2\left(M_1^2 + 2M_1L_2\right) \end{bmatrix} \\ x_4 \\ \dfrac{A}{4m\mu_0}\begin{bmatrix} i_1^2\left(L_1^2 - 2M_2^2 - 2L_1M_2\right) + \\ 2i_1i_2\left(L_1M_1 - 2L_2M_2 - L_1L_2 - M_1M_2\right) + \\ i_2^2\left(M_1^2 - 2L_2^2 - 2M_1L_2\right) \end{bmatrix} \end{bmatrix} \tag{15}$$

Where L_1, L_2, M_1, M_2 are functions of x and y from (5).

System (14) with two inputs and two outputs has the relative degree 2 in a neighborhood of $\mathbf{x} = [0 \quad 0 \quad 0 \quad 0]$ and it is input-state liniarizable.

Feedback linearization of the nonlinear system (14) requires finding a coordinate transformation and feedback by designing the input in such a way the new closed-loop system to be linear and controllable. The new input we choose is the force vector, $\mathbf{F} = [F_x, F_y]^{\mathrm{T}}$ and we developed an equation set which made the transformation:

$$\mathbf{i} = \Psi(\mathbf{x},\mathbf{F}) \tag{16}$$

The transformation (16) was developed as follows:

Magnetic fields in air gaps B_1, B_2, B_3 are calculated by solving (12) and taking account the magnetic coupling, $B_1 + B_2 + B_3 = 0$, the results are the following (only positive values are considered, their sign beeing asinged by a logical function):

$$\begin{aligned} B_1 &= \sqrt{\frac{2\mu_0}{3A}\left[2\sqrt{F_x^2 + F_y^2} + 2F_y\right]} \\ B_2 &= \sqrt{\frac{2\mu_0}{3A}\left[2\sqrt{F_x^2 + F_y^2} + F_x\sqrt{3} - F_y\right]} \\ B_3 &= \sqrt{\frac{2\mu_0}{3A}\left[2\sqrt{Fx^2 + Fy^2} - Fx\sqrt{3} - Fy\right]} \end{aligned} \tag{17}$$

Though there are necessary only the equations for B_1 and B_2, a logical function was built based on this system in order to assign the signs for the magnetic fields, so the currents will have the correct sign to maintain (3). There are serveral possibilities to assign signs to magnetic fields, but we are going to present only one possibility.

Here only positive values of roots are considered. In the first step, at time "zero", the magnetic field which has greatest value is considered positive, and the other two has negative sign in order to maintain $B_1 + B_2 + B_3 = 0$. After this first assignment the signs remain unchanged until a new magnetic field will have the maximum value of three fields. The new maximum field and the old one remains with the same sign and the other magnetic field changes its sign.

With the values of magnetic fields calculated (17), and their signs assigned, the currents are obtained from (1) and (13) as follows:

$$\begin{aligned} i_1 &= \frac{1}{3\mu_0 N}\left[-2B_1g_1 + B_2g_2 + \left(-B_1 - B_2\right)g_3\right] \\ i_2 &= \frac{1}{3\mu_0 N}\left[B_1g_1 - 2B_2g_2 + \left(-B_1 - B_2\right)g_3\right] \end{aligned} \tag{18}$$

Where air gaps between rotor and poles g_1, g_2, g_3 depend on x and y according to (2).

Equations (17), (18) and (2) develop the transformation (16). Equations (18) insure the cancellation of nonlinear block (4) in Fig. 4 and equations (17) together with the logical function insure the decoupling of block (12)+(13). The block diagram of feedback linearization is the following:

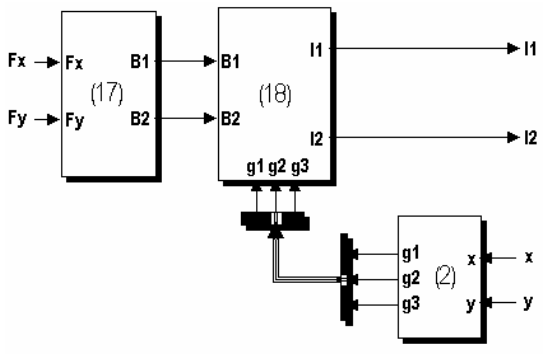

Fig.5 Block diagram of feedback linearization

Using (16) in nonlinear system (14), this is transformed in a closed-loop linear system as follows:

$$\dot{\mathbf{x}} = f(\mathbf{x},\mathbf{i}) = f\left(\mathbf{x},\Psi(\mathbf{x},\mathbf{F})\right) = f\left(\mathbf{x},\mathbf{F}\right) = \mathbf{A}\cdot\mathbf{x} + \mathbf{B}\cdot\mathbf{F} \tag{19}$$

Where **A, B** matrixes are controllable:

$$\mathbf{A}=\begin{bmatrix}0&1&0&0\\0&0&0&0\\0&0&0&1\\0&0&0&0\end{bmatrix},\ \mathbf{B}=\begin{bmatrix}0&0\\1/m&0\\0&0\\0&1/m\end{bmatrix} \tag{20}$$

The linear system also allows the decoupled control on horizontal and vertical axes.

V. Control of the 3-pole AMB

A. PD control – linear control

For x direction the linear system (19) is:

$$\begin{cases}\dot{x}_1=x_2\\ \dot{x}_2=(1/m)\cdot F_x\end{cases}\Leftrightarrow\begin{bmatrix}\dot{x}_1\\ \dot{x}_2\end{bmatrix}=\begin{bmatrix}0&1\\0&0\end{bmatrix}+\begin{bmatrix}0\\1/m\end{bmatrix}F_x \tag{21}$$

This system has a simple form and a PD controller or a state feedback control is the usual control for this system. In fact, in our case, when the desired position is $x^*=0$, the PD controller is the same with the state feedback control and parameters of the state feedback are the same with prortional and derivative parameters of the PD controller. Controller parameters were calculated using root locus method and desired pulsation of the system was chosen according with the desired speed of the shaft because the vibrations, which give the resistive force F_{Rx} in our model, are proportional with the speed of the shaft. The control in y axis is identical with the one in x axis. The block diagram of the control is the following:

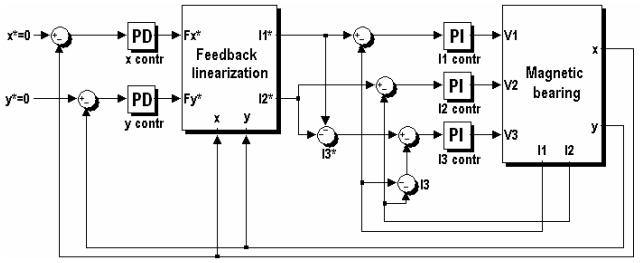

Fig. 6 Block diagram of the PD control of 3-pole AMB

B. Sliding Mode Control – nonlinear control

The model of the 3-pole AMB has some uncertainties, like parameter variations, external disturbances and unmodelled dynamics, which are not taking account. Thus feedback linearization is not perfect for real systems and the linear control based on feedback linearization is possible not to achieve the best results.

A robust control is necessary to avoid system uncertainties and we used a SM Control (see [2], [6]). As the system (19) is decoupled, two identical sliding mode controllers have been designed, one on each Cartesian axe. Theoretical and practical considerations about SM Control can be found in [3], [4] and [8].

In order to describe the control, the liniar system in x direction (21) is considered.

The standard sliding manifold for this system is:

$$s=x_2+ax_1 \tag{22}$$

The control law must guarantee that the system trajectory intercepts sliding surface $s=0$, in finite time and remains there for all the subsequent time. Once in the sliding surface the system progresses in a reduced dynamic mode called sliding mode. The equations for the sliding mode are system equations reduced to the sliding surface (22), and give the following 1st order differential equation:

$$\dot{x}_1=-ax_1 \tag{23}$$

The solution of (23) is:

$$x_1(t)=x_0\exp(-at) \tag{24}$$

Where x_0 represents the interception point at t=T$_0$ and parameter a must be positive to insure the correct behavior of the system inside the sliding surface.

The next step is to design the control law. A Lyapunov method provides a natural setting for analysis. Stability to the sliding surface requires selecting a generalized Lyapunov function $V(s,x,t)$ which is positive definite and has a negative time derivative. Let this function be:

$$V(s,x,t)=s^2/2 \tag{25}$$

which is clearly positive definite. The time derivative yields:

$$\dot{V}=s\dot{s}=s(\dot{x}_2+a\dot{x}_1)=s\left[(1/m)F_x+ax_2\right] \tag{26}$$

The control law to insure that (26) is negative for all values of s and x_2 is the following:

$$F_x=-m\cdot a\cdot x_2-K\cdot\mathrm{sgn}(s)\quad K>0 \tag{27}$$

There are only two parameters to chose in order to impose the behavior of the system. The first one a, is the time constant of a first order system. The second one K, has relation with how rapidly the system intercepts the sliding surface. Their values were selected by simulation in order to provide similar results with the linear control.

Fig. 7 shows the block diagram of the sliding mode controller for x axis:

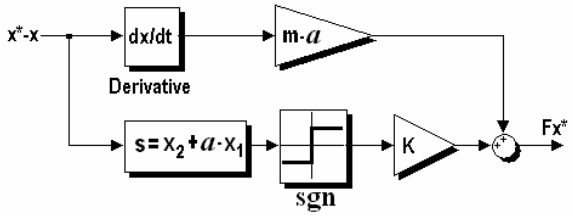

Fig. 7 Block diagram of the sliding mode controller

A control smoothing approximation is made by replacing sgn(s) function with sat(s/ε) function (ε>0) defined by:

$$sat(s)=\begin{cases}\text{sgn}(s) & if \quad |s|\geq\varepsilon \\ s/\varepsilon & if \quad |s|<\varepsilon\end{cases} \tag{28}$$

This approximation is used to avoid control chattering around the operating point and the parameter ε is the one which controls this behavior.

The sliding mode controller for y direction is identical, and the block diagram of the control is similar with the one presented in Fig. 6.

VI. Comparison between controls

Feedback linearization is a strong tool so PD Control has very good results. Simulations proved significant improvement when feedback linearization was used instead of linearization around operating point – in both cases we used the same PD control.

A comparison between the PD control and SM Control applied on the system using feedback linearization is difficult. Both controls have strong and weak points and the purpose of the study is to obtain the best solution for high speeds of the shaft. In order to compare them, we tuned both controls (in simulations) to achieve almost the same time response with almost the same small overshoot at the step input (Fig. 8a). This may be a method to tune sliding mode controllers because there is no algorithm to tune them similar to linear controllers. With these parameters of the controllers, the results of different simulated and experimental tests were compared.

Simulations proved that SM Control is better for parameters variation and PD Control is better for noisy signals, but the difference between results is quite small (Fig. 8b).

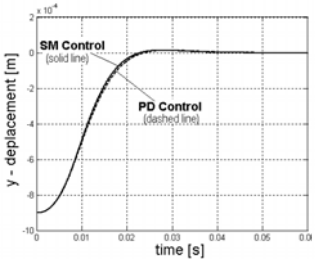

Fig. 8a Step response of both controls

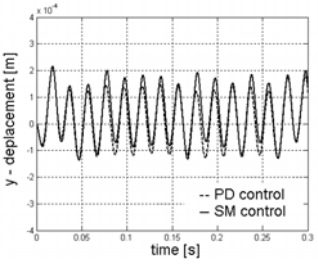

Fig. 8b Controls with noisy signals for position information

Experimental tests with the flywheel confirmed good simulated results for both controls and SM Control had better results because of the nonlinearities of the real system, but again the difference between results is small. The system was tested with zero speed of the shaft and low speeds (1500rpm). For the highest speed of the rotor we had, the duty cycle of the shaft was small and we expect to achieve high speeds with this system – Fig. 9. Both controls remain valid to be tested at high speeds in order to decide the appropriate one.

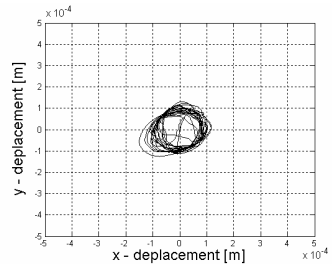

Fig. 9 Shaft position at 1500rpm

References

[1] S.-L. Chen, C.-T. Hsu, "Optimal design of a three-pole active magnetic bearing," IEEE Trans. Magn., vol. 38, no. 5, pp. 3458-3466, September 2002

[2] S.-L. Chen, S.-H. Chen, S.-T. Yan, "Experimental validation of a current-controlled three-pole magnetic rotor-bearing system," IEEE Trans. Magn., vol. 41, issue 1, part 1, pp. 99-112, January 2005.

[3] D. Cho, Y. Kato, D. Spilman, "Sliding mode and classical controllers in magnetic levitation systems," IEEE Control Systems Magazine, vol. 13, issue 1, pp. 42-48, February 1993.

[4] R.DeCarlo, S. Zak, G. Matthews, "Variable structure control of nonlinear multivariable systems: a tutorial," Proceedings of the IEEE, vol. 76, no. 3, pp.212-232, March 1988.

[5] W. Hofmann, "Behaviour and control of an inverter-fed three-pole active radial magnetic bearing," ISIE 2003, CD- ROM, June 2003.

[6] C.-T. Hsu, S.-L. Chen,"Nonlinear control of a 3-pole active magnetic bearing system," Automatica, vol. 39, issue 2, pp. 291-298, February 2003.

[7] L. Li, "Linearizing magnetic bearing actuators by constant current sum, constant voltage sum, and constant flux sum," IEEE Trans. Magn., vol. 35, no. 1, pp. 528-535, January 1999.

[8] V.I. Utkin, "Variable structure systems with sliding modes," IEEE Trans. Automatic Contorl, vol. AC-22, no. 2, pp. 212-222, April 1977.